Equations of state for bicritical points. III. Cubic anisotropy and tetracriticality

Eytan Domany* and Michael E. Fisher
Laboratory of Atomic and Solid State Physics and Baker Laboratory, Cornell University, Ithaca, New York 14853
(Received 3 November 1976)

Crossover scaling functions for a two-component spin system with quadratic anisotropy g and cubic anisotropy $\tilde{v}$ are calculated to first order in $\epsilon = 4-d$ and in $\tilde{v}$, near the transitions within the ordered phases below the multicritical point ($T = T_m, g = 0$). Emphasis is placed on the mechanism by which the system is driven to bicritical or tetracritical behavior by the dangerous irrelevant variable $\tilde{v}$. Explicit expressions and graphs for the various thermodynamic scaling functions are presented.

I. INTRODUCTION

In two previous papers,[1,2] henceforth referred to as I and II, the crossover scaling functions of an n-component spin system with a bicritical (or tetracritical) point were calculated, to first order in $\epsilon = 4-d$, for the disordered phase (in I) and for the Ising-like ($m = 1$) ordered phases (in II). However, the calculations presented in II lose validity asymptotically as the vicinity of the flop line is approached (i.e., near the transition line *in* the ordered phase). Here we present calculations of various thermodynamic functions for a two-component ($n = 2$) system, that are valid in this previously excluded region.

Physical systems described by the present study include uniaxial antiferromagnets like $GdAlO_3$,[3] and the planar ordered or XY-like antiferromagnets, such as Cr_2TeO_6,[4] and $KCuF_3$. Since experimental data of increasing accuracy are becoming available for these systems,[3,4] we believe that the various scaling functions obtained here will be of both theoretical and experimental interest.

As in I and II we consider a Landau-Ginzburg-Wilson–type Hamiltonian but with the addition of a term of cubic symmetry, specifically

$$\mathcal{H} = -\int d\vec{R}\{\tfrac{1}{2}[(\vec{\nabla}s_{\parallel})^2+(\vec{\nabla}s_{\perp})^2 + r_0(s_{\parallel}^2+s_{\perp}^2) - \tfrac{1}{2}g_0(s_{\parallel}^2-s_{\perp}^2)] + u_0(s_{\parallel}^2+s_{\perp}^2)^2 + \tilde{v}_0 s_{\parallel}^2 s_{\perp}^2\}, \quad (1.1)$$

where $\tilde{v}_0$ is the amplitude of the cubic term[5] which breaks the n-component isotropy even when the quadratic anisotropy parameter g_0 vanishes. As has been pointed out by various authors,[6,7] the stable fixed point (when $g_0 = 0$) is isotropic, with $\tilde{v}^* = 0$ provided $n < n^{\times}(d) = 4 - O(\epsilon)$. Thus $\tilde{v}$ is irrelevant in the regime of interest to us here: however, it must be classified as a *dangerous* irrelevant variable.[8] Its effect is most prominant in the ordered phase, near the region of quadratic isotropy (small g_0). As demonstrated by Bruce and Aharony,[9] and by Mukamel,[4] the system will exhibit either bicritical or tetracritical behavior, according to the sign of $\tilde{v}_0$. For $\tilde{v}_0 > 0$ bicritical behavior is expected but for $\tilde{v}_0 < 0$ tetracritical. This result is also given by mean-field theory[9,10]; however, mean-field theory predicts an incorrect shape of the tetracritical lines (see Fig. 1). The

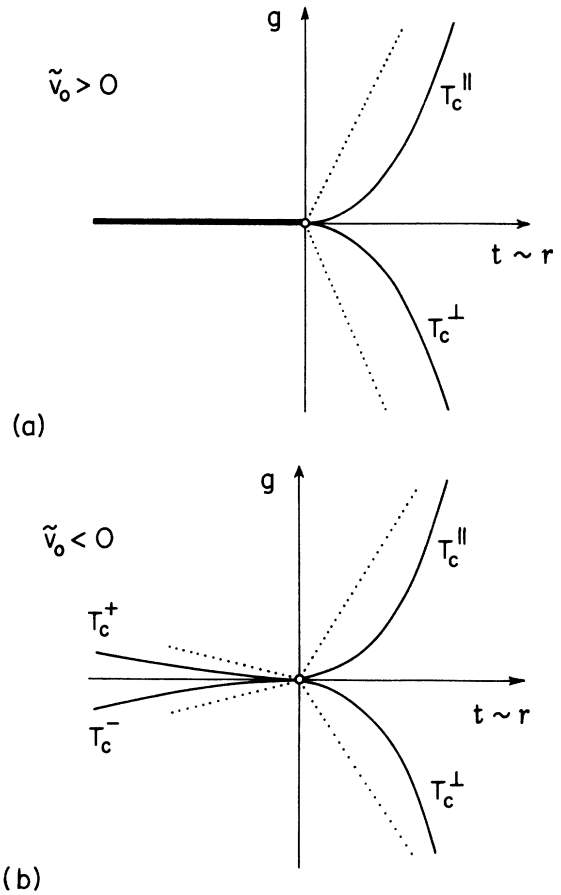

FIG. 1. Bicritical (a) and tetracritical (b) phase diagrams with $t = (T-T_m)/T_m$, where T_m is the multicritical temperature, while g is the anisotropy parameter. The dotted lines indicate the mean-field predictions.

correct form of these critical lines was obtained by Bruce and Aharony[9] who used scaling arguments and Feynman-graph expansions. However, the associated scaling functions have not been calculated previously.

It is of interest to note,[4] that when an antiferromagnet is viewed in a space of the uniform magnetic field $\vec{H}=(H_{\parallel},H_{\perp})$, and temperature T, one can obtain for a given system (i.e., fixed $\tilde{v}_0$) both bicritical and tetracritical behavior, as illustrated in Fig. 2. The present calculation is limited to the dotted planar regions of Fig. 2.

The cubic term plays an additional important role which is independent of the bicritical nature of the problem. For $n=2$, $g_0=0$, and $\tilde{v}_0=0$ we obtain an isotropic XY system. Since there are no ordering fields present in (1.1) the system below the multicritical point T_m is on the coexistence surface (in the full space that includes ordering fields). However, isotropic systems with $n\geq 2$ possess singularities at the coexistence surface[11] associated with spin wave or Goldstone modes. These have been treated by Nelson.[12] We will encounter the effects of these singularities as the flop line is approached in the bicritical case: however, the incipiently divergent fluctuations will be damped by the presence of the anisotropic cubic term and no singularities actually appear for nonzero $\tilde{v}_0$.

Our analysis differs significantly from that of Nelson[12]; while he combined trajectory methods with parquet-graph summation techniques, we have been able to obtain the results using only trajectory integral methods.

The techniques of calculations used in this paper are similar in spirit to those of I and II. However,

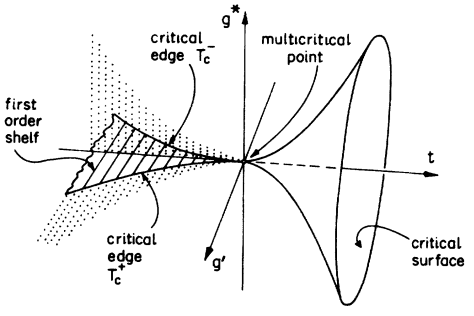

FIG. 2. Three-dimensional phase diagram with one tetracritical planar section and many bicritical sections. For fixed-positive cubic anisotropy $\tilde{v}$, the second quadratic anisotropy field g' may be taken as coupling to a cross term $s_{\parallel}s_{\perp}$ in (1.1). In application to a cubic antiferromagnet (Ref. 4), g corresponds to $(H_{\parallel}^2-H_{\perp}^2)$, while g' corresponds to $(H_{\parallel}^2+H_{\perp}^2)$. Our present results apply asymptotically in the planar regions shown dotted.

the presence of an additional operator requires the solutions of certain differential equations that were not previously handled.

In our discussion we treat the cubic term as a small parameter.[13] Thus the various scaling functions are derived to first order in $\epsilon=4-d$, and first order in $\tilde{v}_0$. This limitation should not be serious in many practical cases where the cubic terms are indeed relatively very small.

Even with this approximation the analysis is quite involved technically. A short discussion based on scaling assumptions is presented in Sec. II as a preview of the form the results must take. The final expressions for the various crossover scaling functions are presented in Sec. V, to which some readers may prefer to proceed directly. Section III summarizes the solutions of the differential equations generated by the renormalization-group procedure. The matching conditions and the reduced Hamiltonian are derived in Sec. IV A, while the matching relations for various thermodynamic functions are given in Sec. IV B. Section VI summarizes the results.

II. SCALING ANALYSIS OF MULTICRITICALITY

We are interested in a system described by the Hamiltonian (1.1), asymptotically close to the multicritical point.[14] The temperaturelike scaling variable will be

$$t\propto r_0-r_{0c}\approx r_0+a_1u_0+a_2\tilde{v}_0. \tag{2.1}$$

As usual $t=0$ and $g_0=0$ locates the multicritical point. In this work we are interested in the ordered region $t<0$. Later on we shall make a specific choice for u_0, so that we need consider only the additional scaling variables $\tilde{v}=\tilde{v}_0$ and $g=g_0$. (We will assume $g_0\geq 0$, with no loss of generality since $n=2$.) The scaling or homogeneity assumption for the singular part of the free energy takes the form[14]

$$f(t,g,\tilde{v})\approx b^{-d}f(b^{\lambda_1}t,b^{\lambda_2}g,b^{\lambda_3}\tilde{v}), \tag{2.2}$$

where λ_1, λ_2, and λ_3 are the appropriate scaling exponents. With the choice $b=|t|^{-1/\lambda_1}$ this takes the form

$$f(t,g,\tilde{v})=a|t|^{2-\alpha}W(z,y), \tag{2.3}$$

where, as usual $2-\alpha=1/\lambda_1$ with α being the XY-like specific-heat exponent, while

$$z=A_1g_0/|t|^{\phi},\quad \phi=\lambda_2/\lambda_1>0, \tag{2.4}$$

$$y=A_2\tilde{v}/|t|^{\phi_v},\quad \phi_v=\lambda_3/\lambda_1<0, \tag{2.5}$$

and $W(z,y)$ is the scaling function of interest. The scale factors a, A_1, A_2 are nonuniversal, and in higher order vary analytically with t, g, etc. [We may choose to normalize by $W(0,0)=1$, $(\partial W/\partial z)_0$

$=1$, etc.] We must note that $\tilde{v}$ is irrelevant; as such, one would expect, asymptotically close to the multicritical point, to have

$$W(z,y)\approx W(z,0), \tag{2.6}$$

with $\tilde{v}$ entering only through the various scale factors. However, since $\tilde{v}$ is a *dangerous* irrelevant variable the asymptotic equality (2.6) fails for the derivatives of $W(z,y)$. Thus, we have to formulate the scaling hypothesis with $\tilde{v}$ explicitly displayed. For $\tilde{v}>0$ we expect bicritical behavior, and for $\tilde{v}<0$ tetracritical. This will be obtained if $W(z,y)$ has a singularity on a locus in the (z,y) plane, given by some equation

$$x = X(z,y) = 0, \tag{2.7}$$

which has no solution for $y>0$ (or $\tilde{v}>0$).

For small z,y we expect an expansion of this equation of the form

$$z + Cy^{\theta} \approx 0. \tag{2.8}$$

Our calculations show that $\theta = 1$, which, in turn, implies that the critical locus can be characterized by an exponent ψ through

$$g \sim |t|^{\psi}, \quad \psi = \phi + |\phi_v|. \tag{2.9}$$

Thus we expect the free energy to have the form

$$f(t,g,\tilde{u}) \approx a t^{2-\alpha}[x^{2-\dot{\alpha}} W_1(z,y) + W_2(z,y)], \tag{2.10}$$

which is, in fact, in agreement with our results. (Here α is the Ising-like specific-heat exponent on the critical lines.)

III. RENORMALIZATION-GROUP DIFFERENTIAL EQUATIONS

Our method of calculation is based on the renormalization-group trajectory integral procedure developed by Rudnick and Nelson.[15] The application of the method to bicritical systems has been discussed in detail in I and II. The basic idea is the following: under application of the renormalization-group transformation[16] (generated by integrating out modes with $\vec{q}$ vectors in an infinitesimal shell near $|\vec{q}| = 1$) the Hamiltonian of (1.1) flows in its parameter space. Various thermodynamic functions can be derived once these flows are known. The flows are obtained in practice from approximate solutions of the differential recursion relations, that are accurate to $O(\epsilon)$ as long as the quadratic coefficients $r_{\parallel}$ and $r_{\perp}$ of the renormalized Hamiltonian do not become too large. When either $r_{\parallel}$ or $r_{\perp}$ (assumed to be initially small) become of order unity, the respective spin variables can be integrated out, leaving a *reduced Hamiltonian* that depends only on the remaining (possibly still critical) spin variables. Our convention ensures $r_{\perp} > r_{\parallel}$ initially. In the disordered phase the recursion relations are such that $r_{\perp}(l) \geq r_{\parallel}(l)$, for all l (where l is the continuous variable that describes the extent of renormalization). Thus, in the disordered phase the $s_{\perp}$ spin variables are integrated out. In the ordered phase we can identify two regions that require different treatments. In the vicinity of the paramagnetic critical line the situation is similar to that in the disordered phase. However, in the vicinity of the flop line (or the critical transition lines T_c^+ and T_c^-) the components $s_{\parallel}$ are to be integrated out. This second case is the subject of the present treatment. A more detailed discussion of this point was presented in II.

Since we work in a region where $\langle s_{\parallel} \rangle = M_0 \neq 0$, it is convenient to introduce a shift by defining

$$s_{\parallel} = \sigma + M_0, \tag{3.1}$$

where M_0 is the *exact* parallel spontaneous magnetization. On writing $s_{\perp} = s$ we then obtain

$$\mathcal{H} = -\int d\vec{R}\{C - \tilde{h}\sigma + \tfrac{1}{2}[\tilde{r}_{\parallel}\sigma^2 + \tilde{r}_{\perp}s^2 + (\nabla\sigma)^2 + (\nabla s)^2] + u(\sigma^2+s^2)^2 + \tilde{v}s^2\sigma^2 + w_{\parallel}\sigma^3 + w_{\perp}\sigma s^2\}, \tag{3.2}$$

where

$$\begin{aligned} &r_{\parallel} = r_{\parallel} + 12uM_0^2, \quad \tilde{r}_{\perp} = r_{\perp} + 4uM_0^2 + 2\tilde{v}M_0^2, \\ &w_{\parallel} = 4uM_0, \quad w_{\perp} = (4u + 2\tilde{v})M_0, \\ &C = \tfrac{1}{2}r_{\parallel}M_0^2 + uM_0^4 - hM_0, \\ &\tilde{h} = h - r_{\parallel}M_0 - 4uM_0^3, \\ &r_{\parallel} = r_0 - \tfrac{1}{2}g, \quad r_{\perp} = r_0 + \tfrac{1}{2}g. \end{aligned} \tag{3.3}$$

For convenience we have introduced an ordering field h into (1.1) coupled to $s_{\parallel}$. Applying the momentum shell integration renormalization group now yields the recursion-relations correct to $O(\epsilon)$,

$$\frac{d\tilde{r}_{\parallel}}{dl} = 2\tilde{r}_{\parallel} + 12K_4uq_{\parallel} + K_4(4u+2\tilde{v})q_{\perp} - 18K_4w_{\parallel}^2q_{\parallel}^2 - 2K_4w_{\perp}^2q_{\perp}^2, \tag{3.4}$$

$$\frac{d\tilde{r}_{\perp}}{dl} = 2\tilde{r}_{\perp} + 12K_4uq_{\perp} + 4K_4\tilde{v}q_{\parallel} - 4K_4w_{\perp}^2q_{\perp}q_{\parallel}, \tag{3.5}$$

$$\frac{dw_{\perp}}{dl} = (1+\tfrac{1}{2}\epsilon)w_{\perp} - 12K_4uw_{\parallel}q_{\parallel}^2 - 6K_4\tilde{v}w_{\parallel}q_{\parallel}^2 - 12K_4uw_{\perp}q_{\perp}^2 - 16K_4uw_{\perp}q_{\parallel}q_{\perp} - 8K_4\tilde{v}w_{\perp}q_{\parallel}q_{\perp}, \tag{3.6}$$

$$\frac{dw_{\parallel}}{dl} = (1+\tfrac{1}{2}\epsilon)w_{\parallel} - 36K_4w_{\parallel}q_{\parallel}^2 - 4K_4uw_{\perp}q_{\perp}^2 - 2K_4u\tilde{v}w_{\perp}q_{\perp}^2, \tag{3.7}$$

$$\frac{d\tilde{h}}{dl}=(3-\tfrac{1}{2}\epsilon)\tilde{h}-3K_4 w_{\parallel}q_{\parallel}-K_4 w_{\perp}q_{\perp}\,, \tag{3.8}$$

$$\frac{du}{dl}=\epsilon u-4K_4(10u^2+u\tilde{v}+\tfrac{1}{4}\tilde{v}^2)\,, \tag{3.9}$$

$$\frac{d\tilde{v}}{dl}=\epsilon\tilde{v}-4K_4(12u\tilde{v}+\tfrac{3}{2}\tilde{v}^2)\,, \tag{3.10}$$

where

$$q_{\parallel}=1/(\tilde{r}_{\parallel}+1)\,,\quad q_{\perp}=1/(\tilde{r}_{\perp}+1)\,, \tag{3.11a}$$

and

$$K_4=1/8\pi^2\,. \tag{3.11b}$$

It should be noted that (3.9) and (3.10) are obtained from the recursion relations exact to $O(\epsilon)$ by replacing $q_{\parallel}$ and $q_{\perp}$ by 1: this approximation introduces an error of only $O(\epsilon^2)$ into the subsequent solutions.[1,15] We shall further simplify the analysis by assuming

$$\epsilon^2\ll\tilde{v}_0\ll u_0=O(\epsilon)\,, \tag{3.12}$$

and, as explained, by neglecting terms of $O(\tilde{v}_0^2)$. Then (3.9) and (3.10) reduce to[13]

$$\frac{du}{dl}=\epsilon u-4K_4(10u^2+u\tilde{v})\,, \tag{3.13}$$

$$\frac{d\tilde{v}}{dl}=\epsilon\tilde{v}-48K_4u\tilde{v}\,. \tag{3.14}$$

The solutions of these equations are found to be

$$\tilde{v}(l)=\tilde{v}_0e^{\epsilon l}/Q^{6/5},\quad u(l)=\tilde{u}(l)-\tfrac{1}{8}\tilde{v}(l)\,,$$
$$\tilde{u}(l)=\tilde{u}_0e^{\epsilon l}/Q\,,\quad Q(l)=1+40K_4\tilde{u}_0(e^{\epsilon l}-1)/\epsilon\,, \tag{3.15}$$

as may be checked by substitution. In what follows, we shall choose $\tilde{u}_0=\epsilon/40K_4=u_c$ which eliminates an irrelevant transient, and yields

$$\tilde{v}(l)=\tilde{v}_0e^{-(\epsilon/5)l},\quad u(l)=u_c-\tfrac{1}{8}\tilde{v}(l)\,. \tag{3.16}$$

In solving (3.4) to (3.8) we follow the procedures outlined in II. The solutions, correct to $O(\epsilon)$, obtained this way are

$$w_{\parallel}(l)=4u(l)M(l),\qquad w_{\perp}(l)=[4u(l)+2\tilde{v}(l)]M(l)\,, \tag{3.17}$$

with

$$M(l)=M_0e^{[1-(\epsilon/2)]l} \tag{3.18}$$

and $u(l)$ and $\tilde{v}(l)$ given by (3.16), and

$$\tilde{h}(l)=he^{(3-\epsilon/2)l}-[t(l)-\tfrac{1}{2}g(l)]M(l)-4u(l)M(l)^3$$
$$+K_4[2u(l)+\tilde{v}(l)]M(l)\{1-T_{\perp}(l)\ln[1+T_{\perp}(l)]\}+6K_4u(l)M(l)\{1-T_{\parallel}(l)\ln[1+T_{\parallel}(l)]\}\,, \tag{3.19}$$

$$\tilde{r}_{\parallel}(l)=T_{\parallel}(l)-6K_4u(l)\{1-T_{\parallel}(l)\ln[1+T_{\parallel}(l)]\}-K_4[2u(l)+\tilde{v}(l)]\{1-T_{\perp}(l)\ln[1+T_{\perp}(l)]\}$$
$$+9K_4w_{\parallel}(l)^2\{\ln[1+T_{\parallel}(l)]+T_{\parallel}(l)/[1+T_{\parallel}(l)]\}+K_4w_{\perp}(l)^2\{\ln[1+T_{\perp}(l)]+T_{\perp}(l)/[1+T_{\perp}(l)]\}\,, \tag{3.20}$$

$$\tilde{r}_{\perp}(l)=T_{\perp}(l)-6K_4u(l)\{1-T_{\perp}(l)\ln[1+T_{\perp}(l)]\}$$
$$-K_4[2u(l)+\tilde{v}(l)]\{1-T_{\parallel}(l)\ln[1+T_{\parallel}(l)]\}+2K_4w_{\perp}^2\,\frac{T_{\parallel}(l)\ln[1+T_{\parallel}(l)]-T_{\perp}(l)\ln[1+T_{\perp}(l)]}{T_{\parallel}(l)-T_{\perp}(l)}\,, \tag{3.21}$$

$$T_{\parallel}(l)=t(l)-\tfrac{1}{2}g(l)+12u(l)M(l)^2\,,\quad T_{\perp}(l)=t(l)+\tfrac{1}{2}g(l)+[4u(l)+2\tilde{v}(l)]M(l)^2\,. \tag{3.22}$$

In these results we have introduced

$$t(l)=t_0e^{\lambda_1 l}\,,\quad t_0=r_0+8K_4u_c[1-r_0\ln(1+r_0)]\,,$$

with

$$\lambda_1=2-\tfrac{2}{5}\epsilon\,, \tag{3.23}$$

and

$$g(l)=\bar{g}_0e^{\lambda_2 l}[1-3\tilde{v}(l)/8u_c]\,,\quad \bar{g}_0=g_0(1+3\tilde{v}_0/8u_c)\,,$$

with

$$\lambda_2=2-\tfrac{1}{5}\epsilon\,. \tag{3.24}$$

Note that to leading order we have $\tilde{r}_{\parallel}=T_{\parallel}(l)$ and $\tilde{r}_{\perp}(l)=T_{\perp}(l)$.

These solutions of the recursion relations will be used for $l\leq l^*$, where l^* is determined by requiring that $\tilde{r}_{\parallel}(l^*)$ be of order unity. As will be shown later, $\tilde{r}_{\perp}(l^*)$ can still be small at this matching point. Explicitly the matching condition we will use has the form

$$T_{\parallel}(l^*)=1+O(\epsilon)\,. \tag{3.25}$$

IV. REDUCED HAMILTONIAN AND THERMODYNAMIC FUNCTIONS

A. Reduced Hamiltonian and explicit matching conditions

Since $T_{\parallel}(l^*)$ depends on $M(l^*)$, it is necessary to determine the latter also in solving the matching condition (3.25). This is achieved by recalling that M_0 was chosen as the *exact* magnetization; thus the shifted Hamiltonian must satisfy the relation

$$\langle\sigma\rangle_{\mathcal{H}(l)} = \int_\sigma \int_s \sigma_{\vec{q}=0} e^{\mathcal{H}(l)} \Big/ \int_\sigma \int_s e^{\mathcal{H}(l)} = 0 . \qquad (4.1)$$

To evaluate this condition at $l = l^*$ we first integrate out the noncritical σ components. (We may remark that the present treatment differs from most of our previous work in that the spin variables that are integrated out appear not only in $\mathcal{H}$, but also as the variable whose expectation value is to be calculated. This situation was encountered before only in the calculation of the perpendicular susceptibility $\chi_\perp$, in I and II.) First we define the reduced Hamiltonian by

$$e^{\mathcal{H}_{\rm red}[s]} = \int_\sigma \exp(\mathcal{H}_\parallel[l^*;\sigma] + \mathcal{H}_\perp[l^*;s] + \mathcal{H}_\times[l^*;\sigma,s]) , \qquad (4.2)$$

where $\mathcal{H}(l^*)$ has been decomposed into three kinds of terms according to the dependence on σ only, on s only, or on both s and σ. We also have

$$\mathcal{H}_\parallel[l^*;\sigma] = \mathcal{H}^0_\parallel[l^*;\sigma] + \mathcal{H}^1_\parallel[l^*;\sigma] , \qquad (4.3)$$

where

$$\mathcal{H}^0_\parallel[l^*;\sigma] = -\tfrac{1}{2}[(\nabla\sigma)^2 + \tilde{r}_\parallel(l^*)\sigma^2] . \qquad (4.4)$$

Now we may expand to get

$$e^{\mathcal{H}_{\rm red}[s]} = e^{\mathcal{H}_\perp[l^*,s]} \times \int_s e^{\mathcal{H}^0_\parallel[l^*,\sigma]} \{1 + (\mathcal{H}^1_\parallel[l^*,\sigma] + \mathcal{H}_\times[l^*,\sigma,s]) + \tfrac{1}{2}(\mathcal{H}^1_\parallel[l^*,\sigma] + \mathcal{H}_\times[l^*,\sigma,s])^2 + \cdots\} . \qquad (4.5)$$

The various integrals can be performed and when the contributions are reexponentiated, we obtain an explicit expression for $\mathcal{H}_{\rm red}[s]$. Before carrying this out, however, we shall determine the matching condition based on (3.25) and (4.1).

The condition (4.1) may be expressed diagrammatically as shown in Fig. 3. The solid lines represent the propagators of the σ variables, which are to be integrated; the dot represents the external σ_0. The broken lines represent the s variables; these *remain unintegrated:* the closed loop denotes the last term of Eq. (4.6). Thus we obtain

$$\tilde{h}(l^*) - 3K_4 w_\parallel(l^*) \int_0^1 \frac{q^3 dq}{\tilde{r}_\parallel(l^*) + q^2} - w_\perp \int_0^1 d^4 q \langle s_q s_{-q}\rangle_{\mathcal{H}_{\rm red}} = 0 . \qquad (4.6)$$

By using (3.25) we may replace $\tilde{r}_\parallel(l^*) = T_\parallel(l^*) + O(\epsilon)$ by 1. The third term on the left is simply the energy of the reduced system, given by[17]

$$\frac{1}{2}\int_0^1 dq \langle s_q s_{-q}\rangle_{\mathcal{H}_{\rm red}} = E_s(t_{\rm red}, u_{\rm red}) + \tfrac{1}{4}K_4[1 - t_{\rm red}\ln(1 + t_{\rm red})] ,$$

$$E_s(t_{\rm red}, u_{\rm red}) = -\frac{1}{24 u_{\rm red}} t_{\rm red} \times \left[\left(1 + \frac{36 K_4 u_{\rm red}}{\epsilon}(t_{\rm red}^{-1/2\epsilon} - 1)\right)^{1/3} - 1\right] . \qquad (4.7)$$

If E_s is expanded in powers of ϵ with $u_{\rm red} = O(\epsilon)$ we obtain $E_s = O(1)$; thus any term that has the form uE_s will be of order ϵ. Although we will leave E_s unexpanded, in order to preserve the singularity associated with it, we shall bear this fact in mind in what follows.

Now we substitute $h(l^*)$ from (3.19), with $h = 0$ into (4.6). On performing the integral in the second term of (4.6), and using (4.7) for the third term, we obtain

$$4u(l^*)M(l^*)^2 = -[t(l^*) - \tfrac{1}{2}g(l^*)] + A , \qquad (4.8a)$$

$$A = -8[u(l^*) + \tfrac{1}{2}\tilde{v}(l^*)]E_s(t_{\rm red}, u_{\rm red}) . \qquad (4.8b)$$

To impose (3.25) we recall from (3.22) that

$$T_\parallel(l^*) = t(l^*) - \tfrac{1}{2}g(l^*) + 12u(l^*)M(l^*)^2 = -2[t(l^*) - \tfrac{1}{2}g(l^*)] + 3A , \qquad (4.9)$$

where we have used (4.8) to derive the second equality.

Now we define our matching condition more explicitly by

$$-t(l^*) + \tfrac{1}{2}g(l^*) = \tfrac{1}{2} , \qquad (4.10)$$

which obviously ensures

$$T_\parallel(l^*) = 1 + 3A . \qquad (4.11)$$

Since by the argument that follows (4.7) we have $A = O(\epsilon)$, and $\tilde{r}_\parallel(l^*) = T_\parallel(l^*) + O(\epsilon)$, this matching condition is consistent with (3.25).

We can turn now to the evaluation of the reduced Hamiltonian. It has the form

$$\mathcal{H}_{\rm red} = -\int \tfrac{1}{2}[(\nabla s)^2 + r_{\rm red}\, s^2] + u_{\rm red} s^4 + \text{const.} \qquad (4.12)$$

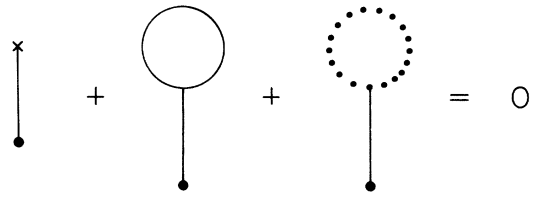

FIG. 3. Diagrammatic representation of relation (4.1). The solid lines represent the propagator associated with σ; the heavy dotted line represents the integral in (4.6); the dots denote the concentraction with the "external" $\sigma_{\vec{q}=0}$ variable.

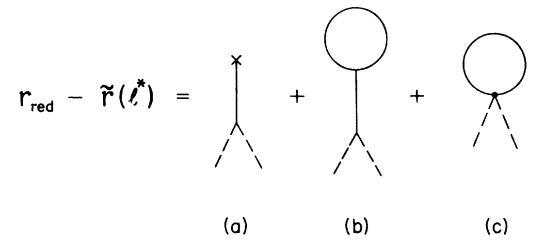

FIG. 4. Diagrams that contribute to r_{red}. The broken lines represent the s variables, and are not integrated, while the solid lines represent the propagator associated with σ.

The diagrams that contribute to r_{red} are shown in Fig. 4, and $r_\perp(l^*)$ is given in (3.21). The third of the diagrams [Fig. 4(c)], exactly cancels the third term on the right-hand side of (3.21). The remaining two diagrams, Figs. 4(a) and 4(b), appear also in Fig. 3 and (4.6), yielding

$$\begin{aligned}(a)+(b) &= \frac{2w_\perp}{T_\parallel(l^*)}\left(\tilde{h}(l^*) - 3K_4 w_\parallel(l^*)\int \frac{q^3\,dq}{T_\parallel(l^*)+q^2}\right)\\ &= 2w_\perp^2(l^*)\int_q \langle s_q s_{-q}\rangle_{\mathcal{H}_{red}}\\ &\cong 4[u(l^*)+\tilde{v}(l^*)]\int_q \langle s_q s_{-q}\rangle_{\mathcal{H}_{red}}\,, \end{aligned} \tag{4.13}$$

where the last equality is correct to $O(\tilde{v})$, and follows from (3.17), (4.8a), and (4.10). Of the various terms in (3.21) we turn now to $T_\perp(l^*)$, as given by (3.22), namely,

$$T_\perp(l^*) = t(l^*) + \tfrac{1}{2}g(l^*) + 4[\tfrac{1}{2}u(l^*)]M(l^*)^2\,.$$

Using (4.8a) and (4.10) gives

$$\begin{aligned}T_\perp(l^*) &= g(l^*) + 2\tilde{v}(l^*)M(l^*)^2 + A\\ &= g(l^*) + \frac{\tilde{v}(l^*)}{4u(l^*)} + A\left(1+\frac{\tilde{v}(l^*)}{2u(l^*)}\right).\end{aligned} \tag{4.14}$$

Finally, substituting in (3.21) and using (4.13), (4.7), and (4.8b) in the equation for r_{red} of Fig. 4, we find

$$\begin{aligned}r_{red} &= g(l^*) + \frac{\tilde{v}(l^*)}{4u(l^*)} + 2K_4[u(l^*)+\tilde{v}(l^*)]\\ &\times\{1 - T_\perp(l^*)\ln[1+T_\perp(l^*)]\} - 6K_4 u(l^*)\\ &\times\{1 - T_\perp(l^*)\ln[1+T_\perp(l^*)]\} + 2K_4 w_\perp^2(l^*)\\ &\times\frac{T_\parallel(l^*)\ln[1+T_\parallel(l^*)] - T_\perp(l^*)\ln[1+T_\perp(l^*)]}{T_\parallel(l^*) - T_\perp(l^*)}\,.\end{aligned} \tag{4.15}$$

Note that the terms containing A cancel exactly.

Now, in order to map onto an Ising-like model and use known results we want[2,15] r_{red} to have the form

$$r_{red} = t_{red} - 6K_4 u_{red}[1 - t_{red}\ln(1+t_{red})] + O(t_{red}^3)\,. \tag{4.16}$$

By comparing with (4.15) we see that the most obvious candidate to play the role of t_{red} is $g(l^*) + \tilde{v}(l^*)/4u(l^*)$. However, we must first identify u_{red}. The four-spin term in the reduced Hamiltonian will contain, in addition to $u(l^*)$, a contribution[12] from the diagram of Fig. 5(a). Thus a four-spin term of the form

$$\begin{aligned}&u(l^*)\int_{qq'q''q'''} s_q s_{q'} s_{q''} s_{q'''}\,\delta(q+q'+q''+q''')\\ &-\tfrac{1}{2}w_\perp(l^*)^2\int_{qq'q''q'''} s_q s_{q'} s_{q''} s_{q'''}\,\frac{\delta(q+q'+q''+q''')}{\tilde{r}_\parallel(l^*)+(q+q')^2}\end{aligned} \tag{4.17}$$

is generated. We may separate the second term into q-independent and q-dependent parts by using the identity

$$1/(r+Q) = 1/r - Q/r(r+Q)\,. \tag{4.18}$$

The q-independent part yields

$$u_{red} = u(l^*) - \tfrac{1}{2}w_\perp^2(l^*)/\tilde{r}(l^*) = -\tilde{v}(l^*) + O(\epsilon^2)\,. \tag{4.19}$$

The q-dependent part is more strongly irrelevant[16]: however, since we want to match r_{red} to the initial form of (4.16), we shall take it into account in an approximate way, namely through the decoupling

$$s^4 \Rightarrow s^2\langle s^2\rangle\,, \tag{4.20}$$

which will further feed into r_{red}. After some minor approximations, this procedure yields r_{red} in the form of (4.16) with

$$t_{red} = g(l^*) + \tilde{v}(l^*)/4u_c\,, \tag{4.21}$$

where u_c is defined just before (3.16), and

$$u_{red} = -\tilde{v}(l^*)\,. \tag{4.22}$$

These relations together with (4.10) fully define $\mathcal{H}_{red}$.

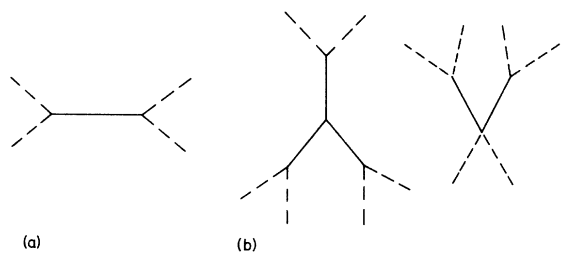

FIG. 5. (a) Diagram that contributes to u_{red}; (b) sixth-order terms (in s) generated by integrating the σ variables.

B. Discussion of $\mathcal{H}_{\rm red}$ and solution of the matching condition

Before going further into the calculation of $t_{\rm red}$ and $u_{\rm red}$, a few general conclusions can already be drawn. The way in which the sign of the irrelevant cubic variable determines the behavior in the ordered phase is revealed by (4.21). We have assumed, (with no loss of generality) that $g_0 \geq 0$. Thus when $\tilde{v}_0 > 0$, $t_{\rm red}$ has a positive lower bound. Thus no critical line (corresponding to $t_{\rm red} = 0$) is expected. However, in this case we also have $u_{\rm red}$ negative; thus we have apparently mapped onto an Ising-like model in the region of a possible first-order transition. Also, keeping only the terms up to fourth order in s seems to have led us from a stable two-component Hamiltonian to an unstable one-component system. However, we have to remember that on integrating out the σ variable, we will also generate terms (of order ϵ^2) of the form $u_6 s^6$ [see Fig. 5(b)]. These terms are positive, and serve to stabilize the reduced Hamiltonian. It is easy to show, that $\mathcal{H}_{\rm red}(t_{\rm red}, u_{\rm red}, u_6)$ lies in the disordered part of the phase diagram; the first order transition occurs when $r_{\rm red} = r_0 \sim u_{\rm red}^2/u_6$; and while our $r_{\rm red}$ is of first order in $\tilde{v}_0$, $u_{\rm red}^2/u_6$ is of order $(\tilde{v}_0)^2$, so that $r_{\rm red} \gg r_0$. This point, and its implications for the scaling functions will be discussed further below.

On the other hand, for $\tilde{v}_0 < 0$ we can map onto a critical one-component system. (The critical point can be approached from the disordered phase.) This, of course, leads to tetracritical behavior, with a critical line given by

$$t_{\rm red} = g(l^*) + \tilde{v}(l^*)/4u_c = 0 . \tag{4.23}$$

Now let us turn back to (4.10) to determine the matching point l^* as a function of t_0, g_0, and $\tilde{v}_0$. Using $t(l)$ and $g(l)$ from (3.23) and (3.24), and $u(l)$, $\tilde{v}(l)$ from (3.16) we get

$$-t_0 e^{\lambda_1 l^*} + \tfrac{1}{2}\bar{g}_0 e^{\lambda_2 l^*}\left(1 - \frac{3\tilde{v}_0}{8u_c} e^{-\epsilon l^*/5}\right) = \tfrac{1}{2} . \tag{4.24}$$

As in Sec. II we define the scaling variables

$$z = \bar{g}_0/t^{\phi}, \quad \phi = \lambda_2/\lambda_1 = 1 + \tfrac{1}{10}\epsilon ,$$
$$y = (\tilde{v}_0/8u_c)\, t^{|\phi_v|}, \quad \phi_v = -\epsilon/5\lambda_2 = -\tfrac{1}{10}\epsilon . \tag{4.25}$$

We require a solution to (4.24) of the form

$$e^{l^*} = (-t_0)^{-1/\lambda_1}\psi(z, y) . \tag{4.26}$$

Substitution yields the equation

$$\psi^{\lambda_1} + \tfrac{1}{2}z(1 - 3y\psi^{-\epsilon/5}) = \tfrac{1}{2} . \tag{4.27}$$

To solve this we represent ψ^2 as

$$\psi^2 = \psi_0^2(1 + 2\epsilon\psi_1 + \cdots)$$

and to first order in y or $\tilde{v}_0$, find

$$\psi_0^2 = (2+z)^{-1}[1 + 3yz/(2+z)] ,$$
$$\psi_1 = -[5(2+z)]^{-1} \times \{\tfrac{1}{2}(2+z)\ln(2+z) - \tfrac{3}{2}zy[1 - \tfrac{1}{2}\ln(2+z)]\} . \tag{4.28}$$

Next we may determine $t_{\rm red}$ and $u_{\rm red}$ from (4.21) and (4.22) as

$$t_{\rm red} = z\psi^{\lambda_2}(1 - 3y\psi^{-\epsilon/5}) + 2y\psi^{-\epsilon/5} , \tag{4.29}$$

$$u_{\rm red} = -8u_c\, y\psi^{-\epsilon/5} = -8u_c\, y + O(\epsilon^2) = -\epsilon y/5K_4 , \tag{4.30}$$

which yields

$$t_{\rm red} = \frac{\tilde{z}[1 + 2y(z-1)/(z+2)]}{(z+2)[1 + O(\epsilon)]} , \tag{4.31}$$

with

$$\tilde{z} = z + 4(2)^{\epsilon/10} y . \tag{4.32}$$

The $O(\epsilon)$ term in (4.31) is lengthy and will not be presented explicitly. Also, in order to keep the various scaling-function expressions tractable, we have, in the amplitudes, dropped terms of order ϵy, keeping only terms of first order in ϵ *and* y.

C. Thermodynamic functions related to $\mathcal{H}_{\rm red}$

(a) The perpendicular susceptibility is defined as

$$\chi_\perp = \int_s\int_\sigma s_0 s_0 e^{\mathcal{H}} \Big/ \int_s\int_\sigma e^{\mathcal{H}} = \langle s_0 s_0 \rangle_{\mathcal{H}} \tag{4.33}$$

and is related to that of the system at l^* by[1,15]

$$\chi_\perp = e^{2l^*}\chi_\perp[\mathcal{H}(l^*)] = e^{2l^*}\chi[\mathcal{H}_{\rm red}] . \tag{4.34}$$

(b) For the parallel susceptibility we likewise have

$$\chi_\parallel = \int_s\int_\sigma \sigma_0\sigma_0 e^{\mathcal{H}} \Big/ \int_s\int_\sigma e^{\mathcal{H}} . \tag{4.35}$$

Although the corresponding formula

$$\chi_\parallel = e^{2l^*}\chi_\parallel[\mathcal{H}(l^*)] \tag{4.36}$$

is still valid, the relation of $\chi_\parallel[\mathcal{H}(l^*)]$ to properties of the reduced Hamiltonian is not simple. A careful diagramatic analysis[18] yields

$$\chi_\parallel(l^*) = 1 + 16[u(l^*) + \tfrac{1}{2}\tilde{v}(l^*)]E_s(t_{\rm red}, u_{\rm red}) + 8[u(l^*) + \tilde{v}(l^*)]C_s(t_{\rm red}, u_{\rm red}) , \tag{4.37}$$

where the energy $E_s(t_{\rm red}, u_{\rm red})$ is given by (4.7), while the specific heat is defined by

$$C_s(t_{\rm red}, u_{\rm red}) = -\frac{\partial E_s(t_{\rm red}, u_{\rm red})}{\partial t_{\rm red}} . \tag{4.38}$$

Thus, we conclude that on approach, in the tetracritical case, to the locus T_c^+, where the s component becomes critical, the susceptibility asso-

ciated with the σ component diverges as an Ising-like *specific heat*. This is to be compared with the analogous behavior near the critical locus $T_c^{\parallel}$; there the susceptibility associated with the noncritical component remained finite, behaving like an Ising-like *energy*.[2]

(c) The spontaneous magnetization M_0 is given by (3.18) as

$$M_0 = e^{-(1-\epsilon/2)l^*} M(l^*),$$

where $M(l^*)$ can be found from (4.8) and (4.10).

(d) The free energy is given, as in II, by the sum of a trajectory integral and the contribution at l^*, namely,

$$F = \text{const} + \int_0^{l^*} e^{-dl} G(l)\, dl + e^{-dl^*} F[\mathcal{H}(l^*)], \quad (4.39)$$

where

$$G(l) = \tfrac{1}{2} K_4 \{\ln[1+\tilde{r}_{\parallel}(l)] + \ln[1+\tilde{r}_{\perp}(l)] - 1\}, \quad (4.40)$$

while the constant term is generated by the shift of $s_{\parallel}$. The calculation of $F[\mathcal{H}(l^*)]$ is achieved by first performing the σ integrals, which leaves the free energy of the reduced Hamiltonian.

The ordinary (nonstaggered) magnetization in the antiferromagnetic interpretation of the model is given by the first derivative of F with respect to g. The second derivative yields the nonordering susceptibility χ_g, while the second derivative with respect to t yields the specific heat. Since the analysis that leads to these functions is rather messy, and differs little from that of II, we quote only the results.

V. THERMODYNAMIC SCALING FUNCTIONS

Our calculations are, in fact, valid to first order in $\epsilon = 4-d$, *and* in $\tilde{v}_0$ independently. For reasons of simplicity, however, we have retained only terms of first order in either ϵ or $\tilde{v}_0$ in the various amplitudes (discarding terms of order $\epsilon\tilde{v}_0$). For convenience we recapitulate here the various variables that enter the scaling functions, expressed in terms of the parameters of the initial Hamiltonian (1.1): these are

$$t = r_0 + 8K_4 u_c [1 - O(r_0^2)], \quad (5.1)$$

$$u_c = \epsilon/40K_4 = u_0 + \tfrac{1}{8}\tilde{v}_0, \quad (5.2)$$

$$\bar{g} = g_0(1 + 3\tilde{v}_0/8u_c). \quad (5.3)$$

The scaling variables are then

$$z = \bar{g}/|t|^{\phi}, \quad \phi = \lambda_2/\lambda_1 = 1 + \tfrac{1}{10}\epsilon, \quad (5.4)$$

$$y = \tilde{v}_0 |t|^{|\phi_v|}/8u_c, \quad \phi_v = -\tfrac{1}{10}\epsilon, \quad (5.5)$$

$$\tilde{z} = z + 4(2)^{\epsilon/10} y, \quad (5.6)$$

while important parts of the scaling functions are

$$\tilde{E}(x,y) = (|x|/24y)\{|x|^{-\epsilon/6}[\tilde{R}(x,y)]^{1/3} - 1\}, \quad (5.7)$$

$$\tilde{C}(x,y) = (1/24y)\{1 - |x|^{-\epsilon/6}[\tilde{R}(x,y)]^{1/3}\}, \quad (5.8)$$

where

$$\tilde{R}(x,y) = (1 + \tfrac{36}{5}y)|x|^{\epsilon/2} - \tfrac{36}{5}y, \quad (5.9)$$

from which one finds

$$\tilde{E}(x,0) = -\tfrac{1}{10}(|x|^{1-(\epsilon/2)} - |x|). \quad (5.10)$$

When $\tilde{v}_0 < 0$, i.e., for $y<0$, the variable $\tilde{z}$ may vanish; in fact, the equation $\tilde{z}=0$ defines the tetracritical line on which Ising-like exponents are observed. The thermodynamic functions then have the following scaling forms:

(a) *Spontaneous magnetization:*

$$M_0^2 = (1/4u_c)|t|^{2\beta}(Q_0 + yQ_1) + O(\epsilon^2, \epsilon y, y^2), \quad (5.11)$$

with

$$Q_0 = 1 + \tfrac{1}{2}z - \tfrac{1}{10}\epsilon(3+2z)\ln(2+z) - \tilde{E}(\tilde{z},y), \quad (5.12)$$

$$Q_1 = 1 - z, \quad \beta = \tfrac{1}{2}(1 - \tfrac{3}{10}\epsilon). \quad (5.13)$$

(b) *Parallel susceptibility:*

$$\chi_{\parallel} = |t|^{-\gamma}(Q_2 + yQ_3) + O(\epsilon^2, \epsilon y, y^2), \quad (5.14)$$

with

$$Q_2 = [1/(2+z)]\{1 - \tfrac{1}{5}\epsilon\ln(2+z) + [2/(2+z)]\tilde{E}(\tilde{z},y) + \tilde{C}(\tilde{z},y)\}, \quad (5.15)$$

$$Q_3 = 3z/(2+z)^2, \quad \gamma = \gamma(n=2) = 1 + \tfrac{1}{5}\epsilon. \quad (5.16)$$

(c) *Perpendicular susceptibility:*

$$\chi_{\perp} = |t|^{-\gamma}\tilde{z}^{-\dot{\gamma}}[\tilde{R}(\tilde{z},y)]^{1/3}(Q_4 + y), \quad (5.17)$$

with

$$Q_4 = 1 - \tfrac{1}{5}\epsilon\ln(2+z), \quad \dot{\gamma} = \gamma(n=1) = 1 + \tfrac{1}{6}\epsilon. \quad (5.18)$$

(d) *Free energy (singular part):*

$$F_s = -\frac{1}{64u_c}|t|^{2-\alpha}\left[(2+z)^2\left(1 + 2y\,\frac{1-2z}{2+z} - \frac{\epsilon}{10}\ln(2+z)\right) + \tfrac{1}{3}z^2[1 - 9y - \tfrac{3}{10}\epsilon\ln(2+z)] + 1 - \tfrac{1}{10}\epsilon\ln(2+z) - \frac{\tilde{z}^2}{6y}\{\tilde{z}^{-\dot{\alpha}}[\tilde{R}(\tilde{z},y)]^{1/3} - 1\} - |t|^{\alpha}\right], \quad (5.19)$$

with

$$\alpha = \alpha(n-2) = \tfrac{1}{10}\epsilon, \quad \dot{\alpha} = \tfrac{1}{6}\epsilon. \quad (5.20)$$

(e) *Nonordering magnetization:*

$$\tilde{M} = -\frac{\partial F}{\partial g_0} = |t|^{\tilde{\beta}} \frac{1}{16u_c}\left(1+\tfrac{2}{3}z - 2y - \frac{5yz}{2} - \frac{\epsilon}{10}(2+z)\ln(2+z) - \frac{\tilde{z}}{8y}\{\tilde{z}^{-\dot{\alpha}}[\tilde{R}(\tilde{z},y)]^{1/3} - 1\}\right), \tag{5.21}$$

with $\tilde{\beta} = 2 - \alpha - \phi$.

(f) *Nonordering susceptibility:*

$$\chi_s = \frac{\partial \tilde{M}}{\partial g_0} = |t|^{-\tilde{\gamma}} \frac{1}{24u_c}\left(1 - \tfrac{15}{4}y - \frac{3\epsilon}{20}[1+\ln(2+z)] - \frac{3}{16y}\{\tilde{z}^{-\dot{\alpha}}[\tilde{R}(\tilde{z},y)]^{1/3} - 1\}\right), \tag{5.22}$$

with $\tilde{\gamma} = 2 - \alpha - 2\phi$.

These results have to be considered in two different cases. When $\tilde{v}_0$ is negative, they apply only for $\tilde{z} \geq 0$ and the various thermodynamic functions exhibit Ising-like singularities on the line $\tilde{z} = 0$.

When $\tilde{v}_0$ is positive, the reduced Hamiltonian has $t_{\text{red}} \geq 0$, with $u_{\text{red}} < 0$. As was discussed in Sec. IV A, the reduced Hamiltonian is, in fact, stabilized by terms of the form $u_6 s^6$. We also have $u_{\text{red}} = O[v(l^*)] = O(\epsilon y)$, with $t_{\text{red}} \geq O(y)$. Thus $\mathcal{H}_{\text{red}}$ corresponds to a single-component Hamiltonian, and since $t_{\text{red}} \gg u_{\text{red}}^2/u_6$ we are in the region of the $(t_{\text{red}}, u_{\text{red}})$ plane that is shaded in Fig. 6. As the bicritical point is approached along the flop line ($z \simeq 0$) the various scaling functions in terms of the reduced variables, degenerate into those of a Gaussian system.[19] However, the divergences of the various susceptibilities on the coexistence lines are again damped by the cubic term; specifically we find from (5.15) and (5.17) the magnitudes

$$\chi_{\parallel} \sim (\tilde{v}_0)^{-\epsilon/2}, \quad \chi_{\perp} \sim (\tilde{v}_0)^{-1} \tag{5.23}$$

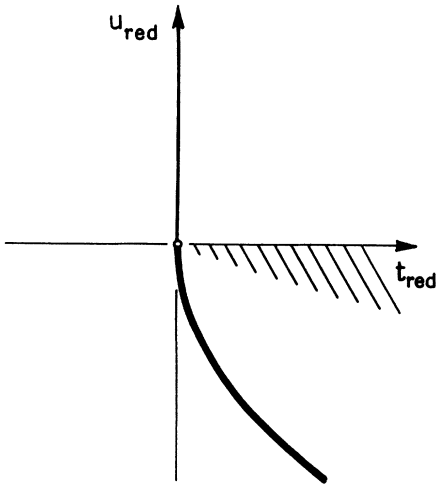

FIG. 6. Phase diagram of an Ising-like system in the (t,u) plane with a line of critical points ($t_{\text{red}} = 0$, $u_{\text{red}} > 0$), and a first-order transition (bold line). The integration over σ maps $\mathcal{H}[s,\sigma]$ onto Hamiltonians $\mathcal{H}_{\text{red}}[s]$, lying in the shaded region.

on the first-order line. This is in agreement with the predictions of Wallace.[20] However, when $\tilde{v} = 0$ ($y = 0$), Gaussian singularities are seen in the limit $g \to 0$ ($z \to 0$) as is evident from (5.10), where the term $|x|^{1-(\epsilon/2)}$ corresponds to a $g^{1-\alpha_G}$ singularity in which $\alpha_G = \frac{1}{2}\epsilon$ is the Gaussian specific-heat exponent. This behavior corresponds, of course, to the isotropic ($n \geq 2$) coexistence curve singularities associated with the so called Goldstone modes (or spin waves).

A graphic appreciation of our results can be obtained by plotting the various scaling functions, evaluated at $\epsilon = 1$, against the variable $z \sim g/|t|^{\phi}$ for fixed y. This corresponds essentially to varying the quadratic anisotropy field at fixed cubic anisotropy and constant temperature below the multicritical point. (However, in a general situation this may not correspond precisely to constant temperature owing to linear and nonlinear corrections to the scaling axes.[21])

Figure 7 displays the variation of the spontaneous order M_0, with z at values of y equal to 0.1 and 0.01 corresponding to bicriticality (dot-dash curves), at $y = 0$ describing limiting isotropic bicriticality (solid curve), and at $y = -0.01$ and -0.1 which corresponds to tetracriticality (dashed curves). The vertical dotted lines represent the critical lines $T_c^+(g)$ marking the transition to the mixed phase which occurs for $y < 0$ at $\tilde{z} = 0$. Note that the plots of M_0 should continue smoothly into the mixed phase but the present calculations do not extend to the mixed phase region. It can be seen from the graphs that the plots for $y = 0$ and $y < 0$ terminate at $\tilde{z} = 0$ with an infinite slope (vertical tangent). This represents the expected Gaussian or Ising-like singularities, respectively. It should be noted, however, that the vertical scale in Fig. 7 is considerably magnified (and excludes the zero) so that these singularities will not be easy to detect experimentally.

Figure 8 shows corresponding plots of the scaling function for the nonordering magnetization $\tilde{M}$ (which would correspond to the ordinary uniform magnetization in the case of an antiferromagnet). The singularities on the phase boundaries $T_c^+(g)$ and $g = 0$ (for the isotropic case) are comparatively

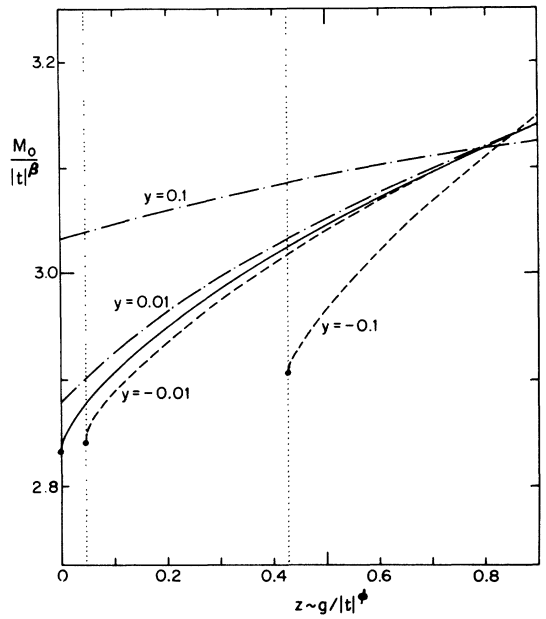

FIG. 7. Scaling function for the spontaneous order M_0 (evaluated at $\epsilon = 1$ as a function of $z \sim g/|t|^{\phi}$ and fixed, scaled cubic anisotropy $y \sim \tilde{v}_0/|t|^{\phi_v} = \tilde{v}_0|t|^{|\phi_v|}$). The dot-dash curves represent bicritical conditions ($\tilde{v}_0, y > 0$); the solid line corresponds to the limiting isotropic case ($\tilde{v}_0 \equiv y \equiv 0$); the dashed curves represent tetracritical situations ($\tilde{v}_0, y < 0$). The dotted vertical lines correspond to the Ising-like critical lines $T_c^{+}(g)$ marking the boundary of the mixed phase regions in the tetracritical case.

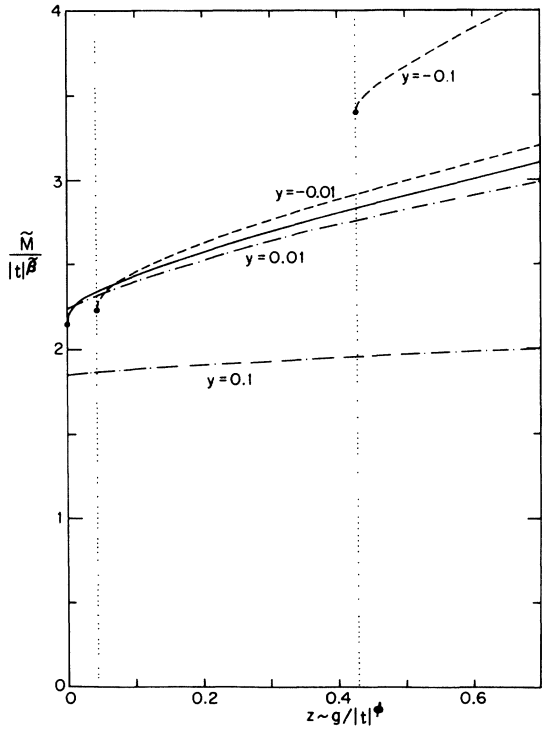

FIG. 8. Scaling function for the nonordering magnetization $\tilde{M}$, at $\epsilon = 1$, as a function of z at fixed y. The solid line represents the isotropic limit, $\tilde{v}_0 \equiv y \equiv 0$.

stronger than in M_0. The visibility of the singularities is improved by differentiation with respect to the anisotropy field g as evident from Fig. 9, which shows the corresponding scaling functions for the nonordering susceptibility χ_g. The divergences correspond to specific-heat-like singularities. The parallel ordering susceptibility $\chi_{\parallel} \sim \partial^2 F/\partial h_{\parallel}^2 \sim \partial M_{\parallel}/\partial h_{\parallel}$ [where $\vec{h} = (h_{\parallel}, h_{\perp})$ is the ordering field], displays on the phase boundaries, singularities of the same character, but of appreciably smaller amplitude. The appropriate plots are displayed in Fig. 10. In the bicritical situation ($\tilde{v}_0, y > 0$) both response functions peak on the first-order boundary, or flop line, but the sharpness of the kink there depends strongly on the value of the cubic anisotropy.

Experimental observations of the variation of the nonordering magnetization $\tilde{M}$ *on* the first order, or flop line in the bicritical situation, offer a direct route to measurement of the crossover exponent ϕ since the exponent for $\tilde{M}(T)$ is $\tilde{\beta} = 2 - \alpha - \phi$.[3,21,22] However, the presence of cubic anisotropy adds a component to the variation of $\tilde{M}(T)$ which could affect such a determination. To gauge this effect we plot in Fig. 11 the effective exponent

$$\tilde{\beta}^*(T) = t \frac{\partial}{\partial t} \ln \tilde{M}(T, g = 0, \tilde{v}_0) \tag{5.24}$$

as a function of

$$\ln y = |\phi_v| \ln|t| + \ln|\tilde{v}_0| + \text{const.}, \tag{5.25}$$

as given by the scaling form with $g \equiv z \equiv 0$. Since

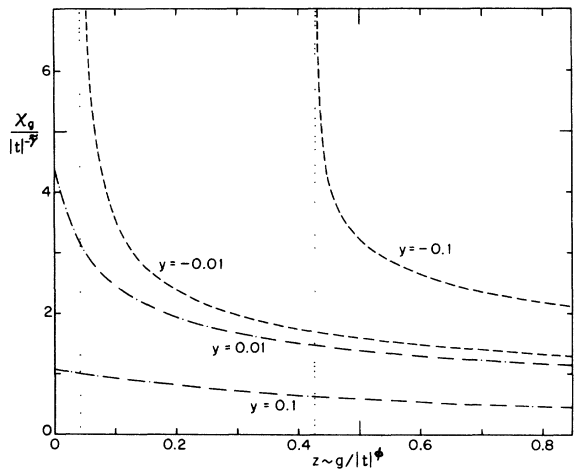

FIG. 9. Scaling function for the nonordering susceptibility χ_g as a function of z at fixed y. The singularities are specific-heat-like.

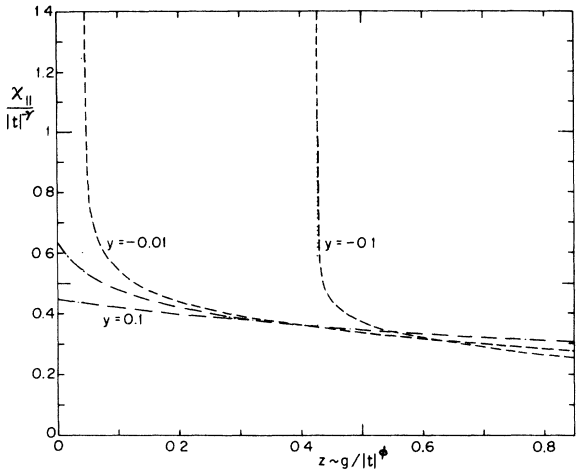

FIG. 10. Plot of the scaling function for the parallel ordering susceptibility $\chi_{\parallel}$ as a function of z at fixed y, displaying weak, specific-heat-like singularities. Note that the parallel spin components are already ordered: it is the perpendicular spin components which are starting to order as the critical line $T_c^+(g)$ is approached (when $\tilde{z} \to 0$).

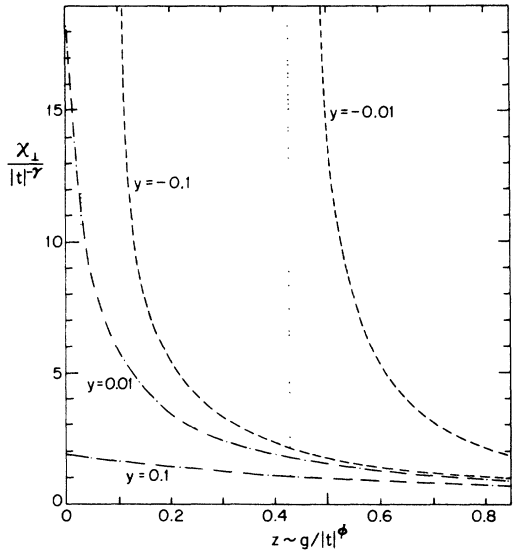

FIG. 12. Plot of the scaling function for the perpendicular ordering susceptibility $\chi_{\perp}$ as a function of z at fixed y, displaying strong Ising-like susceptibility divergences, which correspond to the ordering of the perpendicular spin components which occurs in the mixed phase.

$|\phi_v| \approx \frac{1}{10}\epsilon$ will be small in realistic cases, it can be seen that the effect is not a large one. However, it must be recalled that our result is only valid to first order in $\tilde{v}_0$ and may thus be somewhat misleading for larger values of y.

Finally, Fig. 12 displays the scaling function for the perpendicular susceptibility $\chi_{\perp} \sim \partial^2 F/\partial h_{\perp}^2$ $\sim \partial M_{\perp}/\partial h_{\perp}$. Since the perpendicular spin components described by $M_{\perp}$ are ordering as the critical line $T_c^+(g)$ is approached below T_m, we expect this response function to diverge strongly in the tetracritical cases. Indeed, the exponent of divergence $\dot{\gamma}$ is just the Ising-like susceptibility exponent $\gamma(n=1) \approx 1 + \frac{1}{6}\epsilon$. In the isotropic limit, $\tilde{v}=0$, this goes over to a Gaussian or classical divergence with exponent $\gamma_G = 1$ as can be seen from (5.17).

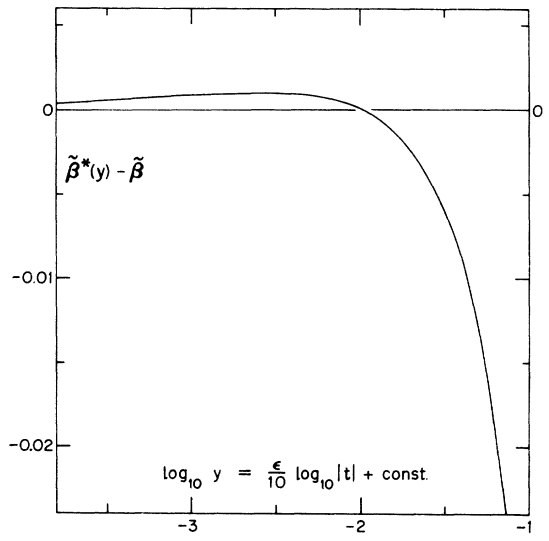

FIG. 11. Plot of the effective exponent $\tilde{\beta}^*(y)$ for the nonordering magnetization relative to its asymptotic value $\tilde{\beta}$ vs $\log_{10} y$, which varies as $(\frac{1}{10}\epsilon \log_{10}|t|$, for $\epsilon = 1 (d=3)$.

VI. SUMMARY

We have extended the calculation of crossover scaling functions in the ordered phases of bicritical and tetracritical systems to the region of small quartic symmetry breaking. This regime is of particular theoretical interest, because of the central role played by a dangerous irrelevant variable.[8] We have clearly demonstrated, in the context of the trajectory integral approach, the mechanism by which such a variable determines the nature of the phase diagram and the thermodynamic functions. Our calculations have yielded explicit crossover scaling functions for various thermodynamic quantities of interest. We expect that these expressions will be useful in analyzing current and future experimental data.

There are various worthwhile extensions of these series of calculations. First, no theoretical results have yet been obtained for the mixed phase (i.e., on the "shelf" in Fig. 2). Second, extension

to the general three-dimensional space of Fig. 2 would be most interesting, since this corresponds to the experimental situation where complete alignment of the fields with appropriate symmetry axes is often very hard to achieve.[3] We hope in the future to undertake studies in these and related directions.

ACKNOWLEDGMENTS

We are grateful for fruitful interactions with Dr. David R. Nelson and Dr. David Mukamel. The support of the NSF, in part through the Materials Science Center at Cornell University, is gratefully acknowledged.

---

*Present address: Dept. of Physics, University of Washington, Seattle, Wash. 98195.

[1]D. R. Nelson and E. Domany, Phys. Rev. B 13, 236 (1976), hereafter referred to as I.

[2]E. Domany, D. R. Nelson and M. E. Fisher, preceding paper, Phys. Rev. B 15, 3493 (1977), hereafter referred to as II.

[3]H. Rohrer, Phys. Rev. Lett. 34, 1634 (1975). We understand that experimental studies on some of the systems discussed here are currently in progress at Brookhaven National Laboratory.

[4]D. Mukamel, Phys. Rev. B 14, 1303 (1976).

[5]We use the tilde notation for the cubic term in (1.1) to avoid confusion with other definitions in the literature, such as

$$u_1(s_\parallel^4+s_\perp^4)+v_1 s_\parallel^2 s_\perp^2 \quad \text{or} \quad u_2(s_\parallel^2+s_\perp^2)^2+v_2(s_\parallel^4+s_\perp^4)\,.$$

[6]A. Aharony, Phys. Rev. B 8, 4270 (1973).

[7]D. R. Nelson, J. M. Kosterlitz, and M. E. Fisher, Phys Phys. Rev. Lett. 33, 813 (1974); E. Brézin, J. C. Le Guillou and J. Zinn-Justin, Phys. Rev. B 10, 892 (1974).

[8]M. E. Fisher, in *Renormalization Group in Critical Phenomena and Quantum Field Theory: Proceedings of a Conference*, edited by J. D. Gunton and M. S. Green (Temple U. P., Philadelphia, Pa., 1974); see also D. R. Nelson, Phys. Rev. B 13, 2222 (1976).

[9]A. D. Bruce and A. Aharony, Phys. Rev. B 11, 478 (1975).

[10]K. S. Liu and M. E. Fisher, J. Low Temp. Phys. 10, 655 (1973).

[11]See, e.g., the recent rigorous work of J. L. Lebowitz and O. Penrose, Phys. Rev. Lett. 35, 549 (1975).

[12]D. R. Nelson, Phys. Rev. B 13, 2222 (1976).

[13]The full equations for u,v to first order in ϵ have been solved exactly by J. Rudnick (private communication).

[14]P. Pfeuty, D. Jasnow, and M. E. Fisher, Phys. Rev. B 10, 2088 (1974).

[15]J. Rudnick and D. R. Nelson, Phys. Rev. B 13, 2208 (1976).

[16]For reviews of the normalization-group method, see K. G. Wilson and J. Kogut, Phys. Rept. 126, 77 (1974); and M. E. Fisher, Rev. Mod. Phys. 46, 597 (1974).

[17]D. R. Nelson, Phys. Rev. B (to be published).

[18]E. Domany (unpublished); D. R. Nelson (Ref. 12) has derived analogous expressions in the presence of an external ordering field (i.e., $h \neq 0$) using a parquet-graph technique. Since he also used different matching conditions, his intermediate results cannot be directly compared with ours.

[19]Gaussian results are obtained by taking the $u_{\text{red}} \to 0$ limit in the various scaling functions: see Ref. 15.

[20]D. J. Wallace, J. Phys. C 6, 1403 (1973).

[21]M. E. Fisher, Phys. Rev. Lett. 34, 1634 (1975).

[22]M. E. Fisher and D. R. Nelson, Phys. Rev. Lett. 32, 1350 (1974).